

Soil microbial community and abiotic soil properties influence Zn and Cd
hyperaccumulation differently in *Arabidopsis halleri*

Priyanka Kushwaha^a, Julia W. Neilson^a, Raina M. Maier^{a*}, Alicja Babst-Kostecka^{a,b*}

^a Department of Environmental Science, The University of Arizona, Tucson, AZ, 85721, USA

^b W. Szafer Institute of Botany, Polish Academy of Sciences, Department of Ecology, Lubicz
46, 31-512 Krakow, Poland

* Both authors contributed equally to this work

Corresponding author:

Alicja Babst-Kostecka

e-mail: ababstkostecka@arizona.edu

1 **ABSTRACT**

2 Soil contamination with trace metal(loid) elements (TME) is a global concern. This has
3 focused interest on TME-tolerant plants, some of which can hyperaccumulate extraordinary
4 amounts of TME into above-ground tissues, for potential treatment of these soils. However,
5 intra-species variability in TME hyperaccumulation is not yet sufficiently understood to fully
6 harness this potential. Particularly, little is known about the rhizosphere microbial
7 communities associated with hyperaccumulating plants and whether or not they facilitate
8 TME uptake. The aim of this study is to characterize the diversity and structure of
9 *Arabidopsis halleri* rhizosphere-influenced and background (i.e., non-*Arabidopsis*) soil
10 microbial communities in four plant populations with contrasting Zn and Cd
11 hyperaccumulation traits, two each from contaminated and uncontaminated sites. Microbial
12 community properties were assessed along with geographic location, climate, abiotic soil
13 properties, and plant parameters to explain variation in Zn and Cd hyperaccumulation. Site
14 type (TME-contaminated vs. uncontaminated) and location explained 44% of
15 bacterial/archaeal and 28% of fungal community variability. A linear discriminant effect size
16 (LEfSe) analysis identified a greater number of taxa defining rhizosphere microbial
17 communities than associated background soils. Further, in TME-contaminated soils, the
18 number of rhizosphere-defining taxa was 6-fold greater than in the background soils. In
19 contrast, the corresponding ratio for uncontaminated sites, was 3 and 1.6 for bacteria/archaea
20 and fungi, respectively. The variables analyzed explained 71% and 76% of the variance in Zn
21 and Cd hyperaccumulation, respectively; however, each hyperaccumulation pattern was
22 associated with different variables. *A. halleri* rhizosphere fungal richness and diversity
23 associated most strongly with Zn hyperaccumulation, whereas soil Cd and Zn bioavailability
24 had the strongest associations with Cd hyperaccumulation. Our results indicate strong
25 associations between *A. halleri* TME hyperaccumulation and rhizosphere microbial

26 community properties, a finding that needs to be further explored to optimize
27 phytoremediation technology that is based on hyperaccumulation.

28

29 **Keywords:** metal accumulation, microbial diversity, plant growth promoting bacteria,
30 pseudometallophyte, soil metal contamination, trace metal(loid) element

31 1. INTRODUCTION

32 Anthropogenic activities such as mining and smelting significantly contribute to the
33 local accumulation of harmful trace metal(loid) elements (TME) levels in the environment.
34 There is a global legacy of contaminated mine tailings that are eroded and transported by
35 wind and water into nearby ecosystems. Smelting additionally results in TME distribution by
36 releasing metal-rich particles into the atmosphere, which are then deposited downwind into
37 local habitats (Balabane *et al.*, 1999). The sustainable management of contaminants
38 associated with mining and smelting of metal ores is regarded as a worldwide challenge that
39 the mining industry faces (Virgone *et al.*, 2018).

40 Establishing a lasting vegetation cover on contaminated sites is considered the best
41 and most permanent way to minimize wind and water erosion and to stabilize mining
42 impacted soils *in situ* (Mendez & Maier, 2008; Ali *et al.*, 2013). Problematically, seed
43 germination and plant growth are often inhibited under TME-rich conditions. Only a limited
44 number of vascular plant species have evolved TME tolerance and are able to survive and
45 reproduce in such environments (Baker, 1987). The majority of TME tolerant plants are
46 labeled “excluders”, because their tolerance is based on minimizing metal(loid) uptake by the
47 roots and limiting transport to shoots. Yet, certain species and populations are able to
48 accumulate TME into above-ground tissues. Among these accumulators, a rare group called
49 “hyperaccumulators” allocates extraordinarily large amounts of a given TME to their foliage,
50 without showing any toxicity symptoms (Baker, 1981; Reeves & Baker, 2000). Importantly,
51 the capacity for metal hyperaccumulation can differ among genotypes of the same plant
52 species (Babst-Kostecka *et al.*, 2018).

53 Hyperaccumulators provide an opportunity to study plant adaptation to extreme
54 environments and they also have potential to be applied in the development of
55 phytoremediation technologies, especially where metal removal or recovery is desired. There

56 is increasing evidence that TME hyperaccumulation depends on a complex set of interactions
57 among soil properties including TME bioavailability, expression of detoxification genes and
58 metal transporters, as well as the plant-associated microbiome (Thijs *et al.*, 2017; Asad *et al.*,
59 2019; Trivedi *et al.*, 2020). Importantly, it is known that plants enrich the rhizosphere with
60 organic root exudates that in turn selectively attract and stimulate the growth of certain
61 microbial taxa (Honeker *et al.*, 2019b; Trivedi *et al.*, 2020). Accordingly, different plant
62 species may have a different rhizosphere microbiome when grown in the same soil, but also
63 plants of the same species may harbor similar microbial communities in different soils
64 (Miethling *et al.*, 2000). Individual plant genotypes further differentiate their rhizosphere
65 communities to best support the physiology, fitness, and improvement of plant responses to
66 environmental stress (Bressan *et al.*, 2009; Micallef *et al.*, 2009; Yeoh *et al.*, 2017; Trivedi *et*
67 *al.*, 2020). Although several studies have reported on these plant-microbial interactions in
68 hyperaccumulating plants, particularly little is known about factors that lead to TME
69 hyperaccumulation in non-metalliferous sites, where the environmental impact of this
70 phenomenon has remained largely neglected (Lodewyckx *et al.*, 2002; Li *et al.*, 2007; Lopez
71 *et al.*, 2017). The rhizosphere-associated microorganisms, including bacteria, archaea, and
72 fungi, are thus very important for their host and can facilitate plant performance and
73 ecosystem functions in many ways (Mendes *et al.*, 2013). In addition, there is evidence that
74 they can enhance the TME-accumulation capacity of plants, thereby increasing TME content
75 in shoot tissues (Farinati *et al.*, 2009; Farinati *et al.*, 2011; Muehe *et al.*, 2015). Therefore,
76 gaining deeper insight in these interactions across diverse soil types (metalliferous and non-
77 metalliferous) is an important step towards further discerning the hyperaccumulation
78 processes (Rosatto *et al.*, 2019).

79 *Arabidopsis halleri* (L.) O'Kane and Al-Shehbaz is considered a model species for its
80 ability to tolerate and hyperaccumulate excessive quantities of zinc (Zn) and cadmium (Cd;

81 Roosens *et al.*, 2008). It can tolerate high TME concentrations in contaminated soils
82 (metallicolous [M] plant populations), but also thrives under natural conditions on
83 uncontaminated soils (non-metallicolous [NM] plant populations). A broad quantitative
84 variation in tolerance and hyperaccumulation of Zn and Cd has been observed in *A. halleri*
85 across this range of environments (Bert *et al.*, 2000; Bert *et al.*, 2002; Talke *et al.*, 2006;
86 Meyer *et al.*, 2010; Stein *et al.*, 2017; Babst-Kostecka *et al.*, 2018). For Zn and Cd,
87 hyperaccumulation has been defined as over 3000 and 100 mg kg⁻¹, respectively (van der Ent
88 *et al.* 2013). Previous work has shown that while Zn and Cd tolerance levels are usually
89 higher in M populations, NM populations on uncontaminated soils accumulate metals more
90 efficiently than M populations on TME-contaminated soils. Thus, extremely high
91 concentrations are found in *A. halleri* shoots, even when the element is present only at low
92 concentration in the soil, indicating active TME foraging (Dietrich *et al.*, 2019). We
93 hypothesize that the associated soil microbiome in this case helps increase both plant TME
94 accumulation capacity and plant fitness in *A. halleri*.

95 In this study, we characterized *A. halleri* rhizosphere-influenced and background soil
96 microbiomes in locations from TME-contaminated and uncontaminated field sites. We
97 selected four plant accessions from Southern Poland, for which different TME
98 hyperaccumulation capacities have recently been reported (Babst-Kostecka *et al.*, 2018;
99 Dietrich *et al.*, 2021). These data were combined with multiple physicochemical soil variables
100 and host-plant traits to test for plant-soil-microbe associations. Based on this setup, following
101 questions are addressed: (1) Are differences in *A. halleri* Zn and Cd hyperaccumulation
102 capacities associated with variation in rhizosphere-influenced microbial community structure,
103 diversity, and richness? (2) Are there specific bacterial, archaeal, or fungal rhizosphere
104 phylotypes that associate with different hyperaccumulation patterns, plant accessions, and/or
105 TME soil contamination? (3) Do the microbial phylotypes differentiating *A. halleri*

106 rhizosphere-influenced and background communities differ between soils from TME-
107 contaminated vs. uncontaminated sites?

108

109 **2. MATERIAL AND METHODS**

110 *2.1 Sampling and climatic data*

111 Four sites with naturally-occurring *A. halleri* were sampled in Southern Poland in late
112 May 2018 (Table 1 and Fig. S1). Two were TME-contaminated sites, defined here as
113 metalliferous (M), at low altitude in the Olkusz region (M_PL22 and M_PL27). Two were
114 uncontaminated, defined here as non-metalliferous (NM); a sub-alpine location at the northern
115 foothills of the Tatra Mts (NM_PL35) and a low altitude location in Niepołomice Forest
116 (NM_PL14). The M sites differed in their history of industrial activity and source of TME
117 contamination. Site M_PL22 was in the vicinity of the Zn smelter of the Bolesław Mine and
118 Metallurgical Plant near Olkusz and site M_PL27 was near an open-pit mine that was closed
119 in 1912 in Galman. Three replicates of both *A. halleri* rhizosphere-influenced and surrounding
120 background soil were collected at each M and NM site. Rhizosphere-influenced (hereafter
121 referred to as rhizosphere) samples were collected by first cutting away the aerial parts of the
122 plant, followed by excavating soil at depth 0 to 15 cm to expose the plant roots. Roots were
123 excised using sterile instruments, placed into a sterile plastic bag, and shaken to separate and
124 collect ~ 50 g of soil that adhered to the roots for DNA analysis (Solís-Dominguez *et al.*,
125 2012). An additional ~ 50 g of soil was sampled from the top 15 cm of the soil profile next to
126 the *A. halleri* roots for geochemical analysis and placed into a plastic bag. To collect
127 background samples at each site, three 5 x 5 m quadrats that were devoid of *A. halleri*
128 vegetation were marked. For each quadrat, five ~ 50 g samples were taken at 10-15 cm depth
129 devoid of visible plant roots (one from each corner and the center) and composited (Reimann
130 *et al.*, 2008). Subsamples for DNA analysis were taken as described by Kushwaha *et al.*

131 (2021). All samples for DNA analysis were immediately placed on ice, transported back to
132 the lab, and stored at -80°C until DNA extraction. Samples for geochemical analysis were
133 stored at room temperature. After collecting the rhizosphere samples, roots and corresponding
134 *A. halleri* shoots were sampled for elemental composition analysis. Shoots and roots were
135 washed, dried at 80°C, and stored at room temperature. Note, that to avoid clonal replicates of
136 *A. halleri* plants, the distance between samples was at least 5m.

137 Monthly precipitation and air temperature data for the period 1997-2016 were obtained
138 from meteorological databases at the Polish Institute of Meteorology and Water Management
139 – National Research Institute (IMGW-NRI). Specifically, data were used from the
140 meteorological station nearest to each of the four study sites (all within 15 km): Igołomia,
141 Kościelisko-Kiry, Maczki, and Olewin meteorological stations for NM_PL14, NM_PL35,
142 M_PL22, and M_PL27, respectively. Three bioclimatic variables were generated from the
143 monthly temperature and precipitation data, averaged from 1997-2016: mean annual
144 temperature (°C), annual precipitation (mm), and length of growing season (days).

145

146 *2.2 Chemical analyses of plant material and geochemical analyses of soil*

147 For elemental composition analysis, 0.5 g of dry-ground plant material was mixed
148 with 10 ml of HNO₃ (69-70%) and HClO₄ (70-72%) 4:1 v/v, left for 24h, and mineralized at
149 290°C (FOSS Tecator Digestor Auto). Total Zn, Cd, Pb, Cu, Fe K, Na, Mg, and Ca
150 concentration was determined using flame or graphic furnace atomic absorption spectrometry
151 (AAS; Varian AA280FS, AA280Z, Agilent Technologies, Santa Clara, USA). Phosphorus
152 concentration was determined by the vanadium-molybdenum method of Barton (1948) using
153 0.5 g of dry-ground material dissolved in HClO₄, mineralized at 290°C and mixed with
154 vanadium-molybdenum mixture and water. Absorbance at 490 nm were read using a Hach-

155 Lange DR3800 spectrophotometer. The Zn, Cd and Pb translocation factors (TF) were
156 determined as the ratio between metal concentration in shoots and roots.

157 Only rhizosphere soil samples were analyzed for pH, electrical conductivity (EC),
158 total nitrogen (TN), total organic carbon (TOC), total carbon (TC), total inorganic carbon
159 (TIC), NO_2^- -N, NO_3^- -N, NH_4^+ -N, available P (P-Olsen), total Zn, Cd, Pb, Cu, Fe, Mg, Ca, K
160 and Na; bioavailable Cd, Pb, Zn, and soil texture. Samples were sieved at 2 mm and dried.
161 Soil pH (ISO 10390) and EC (PN-ISO 11265) were measured in 1:5 (w:v) water suspensions
162 with a Hach HQ40D meter. Total N was determined using the Kjeldahl method; soil was
163 digested in H_2SO_4 with Kjeltabs ($\text{K}_2\text{SO}_4 + \text{CuSO}_4 \cdot 5\text{H}_2\text{O}$; Foss Tecator Digestor Auto)
164 followed by distillation on a Foss Tecator Kjeltac 2300 Analyzer Unit. Total organic C, TC
165 and TIC was determined with a dry combustion analyzer Leco RC-612 (ISO 10694). To
166 analyze NO_2^- -N, NO_3^- -N, and NH_4^+ -N concentrations, soil samples were shaken in water for
167 1 h (1:10, w:v), filtered through cellulose acetate membrane syringe filters (Huang &
168 Schoenau, 1998) and anions in the extracts were determined with an ion chromatograph
169 Dionex ICS-1100, while NH_4^+ -N was determined with Dionex DX-100. P-Olsen was
170 measured with an ion chromatograph (Dionex ICS-1100, Thermo Fisher Scientific) following
171 soil extraction with 0.5 M NaHCO_3 . In order to determine total Zn, Cd, Pb, Cu, Fe, Mg, Ca,
172 K and Na concentrations, ground samples were digested in hot concentrated HClO_4 (FOSS
173 Tecator Digestor Auto) at 288 – 292°C. Extracted elements were analyzed by flame or
174 graphic furnace AAS as described above. Bioavailable fractions of Zn, Cd and Pb were
175 assessed using Diffusive Gradients in Thin-films (DGT) method following the protocol
176 provided by Dietrich *et al.* (2021). Soil texture was determined through a combination of
177 sieving and sedimentation (ISO 11277).

178

179 *2.3 Extraction of nucleic acids, amplicon sequencing and data processing*

180 DNA was extracted from 0.5 g soil using the FastDNA Spin Kit for Soil™ (MP
181 Biomedicals, Solon OH, USA) as modified by Kushwaha *et al.* (2021). Soil samples were
182 thawed on ice prior to extraction. Extracts were purified using DNeasy PowerClean Pro
183 Cleanup kit (Qiagen, Hilden, Germany) to remove inhibitors and the DNA was quantified
184 using a Qubit 2.0 Fluorometer and double stranded DNA (dsDNA) high sensitivity assay kit
185 (Invitrogen, Carlsbad, California, USA). All DNA extraction steps were performed with
186 negative control samples (blanks) containing only reagents. Bacterial/archaeal 16S rRNA
187 gene primers 515F/806R and fungal internal transcribed spacer (ITS) primers ITS1f-ITS2
188 were used for paired-end amplicon sequencing of DNA extracts as described in Walters *et al.*
189 (2016). The purified amplicons from all the samples were pooled in equimolar concentrations
190 and sequenced with a paired-end read length of 2 x 150-bp on the Illumina MiSeq platform.
191 The DNA library preparation and sequencing runs were conducted by the Microbiome Core at
192 the Steele Children's Research Center, University of Arizona.

193 Raw reads were demultiplexed using the idemp tool (<https://github.com/yhwu/idemp>)
194 and bioinformatics analysis was conducted using the DADA2 pipeline (Callahan *et al.*, 2016).
195 Demultiplexed reads were trimmed to the same length of 140 bases for the forward and
196 reverse reads. The paired-end reads were merged using the default overlap of at least 12 bases
197 and then grouped into amplicon sequence variants (ASVs). After removing poor quality and
198 chimeric ASVs, a total of 1,336,123 and 3,353,095 sequence reads remained for the 16S
199 rRNA and ITS genes respectively, with an average of $51,389 \pm 23,065$ (16S rRNA) and
200 $128,965 \pm 81,943$ (ITS) reads per sample. Taxonomy identities were assigned to
201 bacterial/archaeal and fungal ASVs using the SILVA (Quast *et al.*, 2013) and UNITE ITS
202 (Nilsson *et al.*, 2018) databases, respectively. After removal of the contaminants from the
203 ASV tables through comparisons of samples and the blanks, 11,665 and 6,166 ASVs were

204 retained for analysis of bacterial/archaeal and fungal communities, respectively. Taxonomy
205 tables were normalized using a cumulative-sum scaling approach prior to conducting
206 statistical analysis (Paulson *et al.*, 2013). The raw sequencing data for the 16S rRNA gene and
207 ITS obtained in this study have been submitted to the NCBI BioProject number:
208 PRJNA706064.

209

210 *2.4 Statistical analyses*

211 Microbial richness (number of observed ASVs), Shannon diversity index, and
212 community dissimilarity were determined using the *vegan* package (Oksanen *et al.*, 2008).
213 Bray-Curtis distance was used to calculate community dissimilarity and ordination plots were
214 visualized using non-metric multidimensional scaling (NMDS). The differences in richness
215 metrics and Shannon diversity index across site type (M *vs.* NM), location (NM_PL14,
216 NM_PL35, M_PL22, and M_PL27), and sample type (rhizosphere *vs.* background soil) were
217 tested using Wilcoxon and Kruskal-Wallis tests. The differences in microbial community
218 compositions between these groups were examined using nested permutational multivariate
219 analysis of variance (PERMANOVA; Anderson, 2001). The factor *location* was nested within
220 *site type*, and *sample* was nested within *location*. *Location* and *sample* were considered as
221 random factors. Further, a linear discriminant effect size (LEfSe) analysis (Segata *et al.*, 2011)
222 was performed to identify indicator microbial taxa most likely to explain the differences
223 between i) M and NM sites and ii) rhizosphere *vs.* background soils from both M and NM
224 sites (see <http://huttenhower.sph.harvard.edu/galaxy/root>). A logarithmic cutoff value of
225 linear discriminant analysis (LDA) > 2.0 was applied for LEfSe analysis. Additionally, a
226 similarity of percentages (SIMPER) analysis was performed to determine which ASVs
227 contributed the most to the average dissimilarity in microbial community structure between
228 rhizosphere and background soil samples (iterations=1000). SIMPER was conducted

229 separately for samples from M and NM sites. Only ASVs with permutation *p-values* < 0.05
230 are reported. The LEfSe method identifies statistically significant microbial indicators across
231 each group and it weights the uniqueness of the taxon rather than its overall abundance,
232 whereas SIMPER analysis reports the specific ASVs that contribute most to the average
233 dissimilarity between groups and weights the abundance of individual taxa.

234 Non-parametric Kruskal-Wallis analysis was used to test for differences among the
235 four sites with respect to abiotic and biotic soil properties, Zn and Cd shoot concentrations,
236 and root-to-shoot translocation factors. Partial Least Square (PLS) regression was used to
237 investigate the extent to which geography, climate, as well as biotic and abiotic soil and plant
238 parameters explained variation in Zn and Cd hyperaccumulation. PLS is particularly well
239 suited for situations where the number of predictors exceeds the number of observations
240 (Carrascal et al., 2009), as is the case in our study. The PLS was implemented using function
241 `plsreg2` for multivariate cases from the `plsdepot` package in R (Sanchez & Sanchez, 2012).
242 For each element, the analyses were run on two blocks of variables: a matrix of 95 predictors
243 and a matrix of two responses (i.e., Zn shoot concentration and Zn_{TF} for the Zn
244 hyperaccumulation trait; and Cd shoot concentration and Cd_{TF} for the Cd hyperaccumulation
245 trait). The predictors included: six geographic and climatic variables, nine elemental plant
246 shoot concentrations, as well as 25 geochemical and 55 biological properties of corresponding
247 rhizosphere samples. The biological properties included: i) microbial diversity metrics, e.g.,
248 richness, Shannon diversity index, and NMDS axes scores, ii) relative abundance of indicator
249 microbial taxa likely to explain the differences between rhizosphere vs. background soil
250 samples (rhizosphere taxa with LDA > 4.0 as per LEfSe analysis), and iii) relative abundance
251 of microbial taxa that contributed to the average dissimilarity in microbial community
252 structure (permutation *p-values* < 0.05 as per SIMPER) between rhizosphere and background

253 soil samples from M and NM sites. A heatmap of the relative abundance of taxa identified as
254 significantly associated with Zn and Cd hyperaccumulation was generated using ggplot2 in R.

255 It is noted that geographic and climatic data were represented by a single value per
256 population and that each value was replicated for all samples from the same sampling site. In
257 the PLS analyses, the optimal number of components was determined by leave-one-out cross
258 validation. Cumulative R^2 (%) values are provided according to the retained number of
259 components. These values reflect the explanatory power of the components for all dependent
260 variables (cumulative R^2Y) and for all explanatory variables (cumulative R^2X). Predictors that
261 contributed most to the underlying variation in metal hyperaccumulation were identified
262 based on their “Variable Importance in Projection” (VIP) scores. Accordingly, variables with
263 VIP scores greater than 0.8 were considered critical in a given PLS regression model (Farrés
264 *et al.*, 2015). Effect direction and intensity of each variable are specified by the sign and the
265 absolute value of the corresponding standardized and scaled regression coefficients. All
266 statistical analyses were performed using R 3.6.0 (R Core Team, Vienna, Austria) and
267 XLSTAT.

268

269 3. RESULTS

270 Geographic and climatic data for the sampling sites, elemental plant shoot
271 concentrations, and geochemical properties of rhizosphere soil samples are provided in
272 Supplementary Table S1.

273

274 3.1 General characterization of plant Zn and Cd hyperaccumulation

275 All populations, independent of their edaphic origin, accumulated significantly more
276 Zn (Fig. 1A, 1B) and Cd (Fig. 1E, 1F) in shoot than in root tissues. For Zn, the mean Zn_{shoot}
277 concentration was on average twice as high in M than in NM plants (Table S1). Individual

278 values ranged from 2013 mg kg⁻¹ (NM_PL35) to 13,254 mg kg⁻¹ (M_PL27), with only two
279 NM_PL35 samples not reaching the Zn hyperaccumulation threshold (3000 mg kg⁻¹; van der
280 Ent *et al.* 2013). Interestingly, Zn_{shoot} concentrations in NM_PL14 plants did not differ from
281 M populations (Fig. 1A), despite ~80-fold lower total and bioavailable Zn soil concentrations
282 at the NM_PL14 site (Fig. 1D; Table 1). Further, bioavailable Zn soil concentrations were
283 significantly higher at M sites when compared to NM sites (Fig. 1D). For Cd, M plants had on
284 average nine-fold higher Cd_{shoot} concentrations compared to NM plants. While all M plants
285 hyperaccumulated Cd, none of the NM plants met the hyperaccumulation threshold for this
286 metal (100 mg kg⁻¹; van der Ent *et al.* 2013). All NM and M plants had translocation factors
287 (Zn_{TF} and Cd_{TF}) that exceeded one (Fig. 1C, 1G). Overall, Zn and Cd translocation factors
288 were higher in M compared to NM populations; however, the difference was only significant
289 for Cd translocation in NM vs. M_PL27. Similar to Zn soil concentrations, bioavailable Cd
290 soil concentrations were significantly higher at M sites when compared to NM sites; in
291 addition, the NM_PL35 had significantly higher Cd soil concentrations than NM_PL14 site
292 (Fig. 1H).

293

294 3.2 Microbial community diversity and structure

295 When rhizosphere and background soil samples were analyzed together, neither
296 bacterial/archaeal nor fungal richness were significantly different across the four study sites
297 (Fig. 2A, Table S2). In contrast, community ordination analysis showed that site type (M vs.
298 NM) and location (NM_PL14, NM_PL35, M_PL22, M_PL27) explained 26% and 18%,
299 respectively, of the variation in bacterial/archaeal community composition ($p = 0.001$), as
300 well as 18% and 10% of the variation in fungal community composition ($p = 0.001$) (Fig.
301 2B). Overall, in this analysis 44% and 28% of the community variability for bacteria/archaea
302 and fungi, respectively, could be explained by the combination of site type and location.

303 Wilcoxon test revealed no significant variation for the richness and Shannon diversity index
304 for microbial communities between rhizosphere and background soil (Table S2).

305

306 *3.3 Key microbial taxa differentiating rhizosphere and background soil samples*

307 LefSe and SIMPER analyses were conducted to identify defining taxa that
308 differentiate the microbial communities of M and NM soils and their respective rhizosphere
309 and background soil communities. LefSe weights the uniqueness of a taxon within a
310 community, whereas SIMPER weights the relative abundance. Results showed that M sites
311 had four times as many unique bacterial/archaeal ASVs and almost twice the number of
312 fungal ASVs than were found in NM sites (Table 2). As a result of this difference, the
313 rhizosphere and background soil communities were analyzed separately for the M and NM
314 sites. Overall, the analyses showed a higher number of microbial taxa defining the rhizosphere
315 communities than the background soil communities (Table 2). Further, this difference was
316 more pronounced in M sites for which the rhizosphere: background ratio of unique taxa was
317 almost 6 for both bacteria/archaea and fungi. The corresponding ratio for NM sites, was 3 and
318 1.6 for bacteria/archaea and fungi, respectively (Table 2).

319 The threshold on the logarithmic LDA score for discriminative features was set to 4, to
320 evaluate the microbial taxa that were the most prominent in defining the differences between
321 rhizosphere vs. background soils and M & NM sites. Accordingly, seven out of the 40
322 bacterial/archaeal taxa were identified as the top rhizosphere taxa at M sites, whereas
323 rhizosphere taxa at NM sites had only one out of the 24 taxa with LDA > 4.0 (Figure S2;
324 Table 2). The top bacterial/archaeal rhizosphere taxa at M sites included:
325 *Betaproteobacteriales*, *Burkholderiaceae*, *Gammaproteobacteria*, *Nitrosomonadaceae*,
326 *Pseudonocardiaceae*, *Pseudonocardiales*, and *IS-44* (Fig. S2A; Table S3). In contrast, the top
327 rhizosphere taxon at NM sites was only classified up to the bacterial kingdom level (Fig. S2B;

328 Table S3). For M background soil community, the defining taxa belonged to the phyla
329 *Acidobacteria* and *Actinobacteria* (LDA > 4.0). Interestingly, most of the defining NM
330 background soil taxa belonged to *Thaumarchaeota*.

331 At M sites, LEfSe identified 57 fungal taxa in rhizosphere soil that distinguished the
332 rhizosphere community from the background soil community (Fig. S3A; Table S3). The top
333 six fungal taxa that associated with the M rhizosphere community were Ascomycota,
334 including four taxa that belonged to Dothiodemycetes order (LDA > 4.0; Fig. S3A). Although
335 the number of fungal taxa in the M rhizosphere soil community was higher, the number of
336 bacterial/archaeal and fungal taxa with LDA > 4.0 was the same. Ten fungal taxa were
337 identified by LEfSe as related to the background soil at M sites. These fungal taxa included
338 the phyla: Ascomycota, Basidiomycota, Mortierellomycota, and Glomeromycota (Fig S3A).
339 In contrast, only 11 fungal taxa were identified in the NM rhizosphere community and
340 Cantharellales was the only one fungal taxon with LDA > 4.0 (Fig. S3B).

341 As with LEfSe, SIMPER analysis identified more taxa for M soils that contributed to
342 the dissimilarity between rhizosphere and background soils than for the NM soils (Table S4).
343 Twenty-three and 12 bacterial taxa differentiated the rhizosphere community from the
344 background soil communities for M and NM sites, respectively ($p < 0.05$; Table S4). The
345 genus *Pseudomonas* was the most significant taxa defining M rhizosphere samples, whereas
346 the order *Gaiellales* was the most significant in NM samples. Regarding fungal communities,
347 three taxa explained the differences between rhizosphere and background soil communities
348 from M sites and two taxa from NM sites ($p < 0.05$; Table S4). The fungal species *Russula*
349 *depallens* emerged as the most significant for M sites and its contribution towards the
350 dissimilarity between rhizosphere and background soil communities was the highest among
351 all taxa (1.4%). In NM soils, the fungal taxon from the Helotiales order had the highest
352 contribution to the dissimilarity between rhizosphere and background soils.

353

354 *3.4 Abiotic and biotic variables positively related to enhanced Zn and Cd hyperaccumulation*

355 Leave-one-out cross-validation indicated that the optimal number of partial least
356 square (PLS) components for both regression analyses (i.e., performed on either Zn
357 hyperaccumulation or Cd hyperaccumulation traits) was two. These two components together
358 explained 71% and 76% of the variance in Zn and Cd hyperaccumulation, respectively (Fig.
359 3A; Fig. S4). Importantly, as our regression models were based on the same numbers of
360 components, they are fully comparable.

361 For Zn hyperaccumulation, all abiotic and biotic variables together (cumulative R^2Y)
362 and both Zn hyperaccumulation variables together (cumulative R^2X from Zn_{shoot} and Zn_{TF})
363 explained 50% and 47% of variance for the first PLS component and 21% and 11% for the
364 second component, respectively. For Cd hyperaccumulation, cumulative R^2Y and cumulative
365 R^2X (from Cd_{shoot} and Cd_{TF}) explained 58% and 52% of variance for the first PLS component
366 and 18% and 16% for the second component, respectively. To evaluate the importance of
367 each predictor variable in our models, we used the VIP scores from the PLS output.
368 Accordingly, 45 and 47 out of 95 variables were identified as relevant in the Zn and Cd
369 hyperaccumulation PLS regression models, respectively (Table S5). The absolute values of
370 the corresponding beta regression coefficients express the relative strength of these variables
371 in explaining the variance in Zn and Cd hyperaccumulation (Fig. 3B).

372 A striking result from the PLS analysis is that the three out of the four strongest
373 variables that impacted Zn hyperaccumulation (Zn_{shoot} and Zn_{TF}) were fungi-related including:
374 fungal richness, diversity, and the taxa *Humicola* (Fig. 3B). In contrast, none of these fungi-
375 related variables were important for Cd hyperaccumulation. The only important fungi-related
376 variable for Cd was related to Cd_{TF} and in this case, the taxa *Dothideomycetes* was the
377 strongest impacting variable. Interestingly, *Dothideomycetes* was also a strong variable (10th

378 ranked) for Zn_{TF} (Fig. 3B). Other important variables correlated with Zn uptake included plant
379 shoot concentration of Mg and several abiotic variables including NH_4^+ -N, TOC, TC, TN, and
380 Cu. Bacteria were of less importance as variables that impacted high levels of Zn uptake.

381 The results for Cd are in stark contrast to Zn. The strongest variables related to Cd
382 hyperaccumulation were abiotic soil variables and bacteria. Abiotic variables of importance to
383 enhanced Cd_{shoot} concentrations included Cd and Zn bioavailability. Abiotic variables
384 important for the Cd_{TF} included: Cu content, NH_4^+ -N, TOC, and TC. Bacteria related to high
385 levels of Cd uptake included *Kineosporia* and *Lysinmonas* for Cd_{shoot} and *Pseudomonas*,
386 *Devosia*, *Flavobacterium*, and *Crossiella* for Cd_{TF} . Though abiotic factors and bacteria were
387 most important for Cd hyperaccumulation, the exception was that for Cd_{TF} the fungus
388 Dothideomycetes was the most important factor.

389

390 3.5 Abiotic and biotic variables negatively related to Zn and Cd hyperaccumulation

391 Six out of the seven strongest variables that negatively associated with Zn
392 hyperaccumulation (Zn_{shoot} and Zn_{TF}) were the same including: NO_3^- -N, latitude, bacterial
393 taxa *Nitrospira*, *Phenylobacterium*, *Subgroup2*; and fungal taxa Helotiales Incertae sedis (Fig.
394 3B). Interestingly, bioavailable concentrations of Cd, Pb, and Zn along with pH negatively
395 related to translocation of both Zn and Cd. Seven bacteria taxa negatively impacted Cd_{TF} ,
396 whereas Cd hyperaccumulation was related to fungal NMDS axis score and Dothideomycetes.
397 Notably, different nitrogen forms influenced Zn and Cd hyperaccumulation with NO_3^- -N and
398 NH_4^+ -N relating to Zn and Cd uptake, respectively.

399

400 3.6 Key microbial taxa that associated with Zn and Cd hyperaccumulation

401 PLS analysis identified 29 microbial taxa (24 bacteria and 5 fungi) in rhizosphere as
402 significant explanatory variables of Zn and Cd hyperaccumulation in *A. halleri* shoots (Fig.

403 3). Notably, some taxa were associated uniquely with Zn (7) or Cd (11) hyperaccumulation,
404 whereas many were associated with both (11). The vast majority of these 29 taxa were present
405 in the *A. halleri* rhizosphere at M sites, with 27 and 24 taxa linked to the M_PL27 and
406 M_PL22 sites, respectively (Fig. 4). Only 13 of the taxa were found in the NM_PL35 site, but
407 21 taxa corresponded to the NM_PL14 site. Interestingly, there were 10 bacterial taxa that
408 were present at both M sites and one NM site NM_PL14, but not at NM_PL35. The relative
409 abundance of these taxa in NM_PL14 was either comparable or lower than in M sites. The
410 bacterial taxa belonged to five phyla, including *Acidobacteria*, *Actinobacteria*, *Bacteroidetes*,
411 *Nitrospirae*, and *Proteobacteria* and the five fungal taxa were from the Ascomycota phylum
412 (Table S3). There were six bacterial genera (*Actinomycetospora*, *Crossiella*, *Marmoricola*,
413 *Bradyrhizobium*, *Rhodoplanes*, and *Pseudomonas*) that had relative abundance > 0 in the M
414 sites (M_PL22 and M_PL27) but were absent at NM sites (NM_PL14 and NM_PL35) (Fig.
415 4). In contrast, two bacterial genera, *Nitrospira* and *Phelybacterium*, were present exclusively
416 at NM sites.

417

418 4. DISCUSSION

419 4.1 *Arabidopsis halleri* metal hyperaccumulation patterns in M and NM sites

420 As shown recently, the four *A. halleri* populations (two each from M and NM sites) in
421 this study are both genetically similar and in close geographic proximity (Babst-Kostecka *et*
422 *al.*, 2018). Here, we investigated the differences in Zn and Cd hyperaccumulation among
423 these populations. All plants reached exceptionally high concentrations of both Zn and Cd in
424 the shoots at M sites, whereas only Zn was hyperaccumulated at NM locations. These results
425 are congruent with the findings of previous studies on *A. halleri* and underline the constitutive
426 nature of Zn hyperaccumulation and the population-specific character of Cd
427 hyperaccumulation in this species (Bert *et al.*, 2000; Stein *et al.*, 2017; Corso *et al.*, 2018).

428 The evolutionary dynamics of Zn hyperaccumulation by *A. halleri* are particularly
429 interesting, as illustrated by a recent study that associated an increase in Zn
430 hyperaccumulation in the lowland NM population in Niepołomice Forest with the
431 colonization of this location by plants from a former M population (Babst-Kostecka *et al.*,
432 2018). Similarly, in this study, the NM_PL14 population (Niepołomice Forest) accumulated
433 remarkably high Zn concentrations that match the levels found at M locations, even though
434 the soil Zn concentration at the NM_PL14 site was ~80-fold lower compared to M sites.
435 Interestingly, the Niepołomice Forest accessions have reduced neutral genetic variation
436 compared to other NM and M populations from the same geographic region (Babst-Kostecka
437 *et al.*, 2018), which could negatively impact population fitness (Markert *et al.*, 2010). It is
438 thus surprising that these genetically less diverse *A. halleri* plants showed no visible toxicity
439 symptoms even after extremely high Zn accumulation and reached the highest aboveground
440 biomass of all investigated populations from Southern Poland in an earlier study (Dietrich *et*
441 *al.*, 2019). Taken together, these results suggest that soil TME concentration is not the main
442 driver for *A. halleri* Zn hyperaccumulation and led us to consider other possible biotic and
443 abiotic factors that could influence TME uptake. These are discussed in the following
444 sections.

445

446 *4.2 Microbial community dynamics in M and NM soils*

447 Elevated concentrations of TME are known to impact the soil microbial community.
448 In this study, both M and NM sites were characterized by similar levels of microbial richness
449 and diversity, but notable differences in microbial community composition were observed.
450 Similarly, long-term exposure to historic metal-contaminated mine tailings has previously
451 been reported to have weak or no impact on microbial alpha diversity in soils (Gans *et al.*,
452 2005; Bamborough & Cummings, 2009). This was attributed to the local adaptation of

453 microbial communities and the replacement of metal sensitive groups by more tolerant ones
454 (Berg *et al.*, 2012; Azarbad *et al.*, 2015). In terms of microbial community structure,
455 differences in the composition of both bacterial/archaeal and fungal communities in M and
456 NM sites were observed both in the present and previous studies (Tipayno *et al.*, 2018; Xu *et*
457 *al.*, 2019). As suggested above, these differences may be due to the replacement of metal-
458 sensitive with metal-tolerant microbial populations.

459 Not only did metal contamination (M vs. NM sites) affect the structure of
460 bacterial/archaeal and fungal communities differently in this study but the contribution of site
461 type in shaping the community composition was two-fold greater for bacteria/archaea than for
462 fungi. A similar pattern was previously reported by Khan *et al.* (2010) and may be associated
463 with differences in bacterial and fungal activities in M soils (Rajapaksha *et al.*, 2004). Further,
464 phospholipid fatty acid analysis – commonly used to quantify soil microbial responses to
465 environmental stress – has shown positive correlation between soil available Cd and fungal
466 indicators but for bacterial indicators the correlation is a negative one (Shentu *et al.*, 2014).

467 Of particular interest were the observed differences between *A. halleri* rhizosphere and
468 background soil microbial communities from M and NM sites. In particular, the number of
469 microbial taxa defining the rhizosphere was greater than for background soils. This difference
470 was more pronounced in M than in NM sites. One possible explanation for these findings is
471 that *A. halleri* recruits a more unique rhizosphere community from the background soil in M
472 vs. NM sites. This is supported by Honeker *et al.* (2019), who reported a greater number of
473 taxa enriched in *Atriplex lentiformis* rhizosphere in acidic pyritic mine tailings (24
474 rhizosphere taxa vs. 0 bulk taxa) compared to higher pH (5.2-7.8) substrates (15 rhizosphere
475 taxa vs. 3 bulk taxa). Similar observations were derived from comparisons between *A.*
476 *lentiformis* rhizosphere and bulk taxa in compost-amended and unamended pyritic tailings
477 (Valentín-Vargas *et al.*, 2018). Taken together, these findings indicate that plants growing

478 under M conditions recruit a greater number of novel rhizosphere taxa than their counterparts
479 in NM soils.

480 Another possible explanation for a higher number of unique defining rhizosphere taxa
481 in M sites may be the presence of specific metal tolerant or plant growth promoting bacteria
482 (PGPB) that facilitate survival and help alleviate plant metal stress (Ma *et al.*, 2015). Overall,
483 PGPB can enhance plant growth by regulating plant stress responses through the production
484 of siderophores, phytohormones, and enzymes (Penrose & Glick, 2001; Press *et al.*, 2001;
485 Patten & Glick, 2002). The present study identified several bacterial groups with the above-
486 mentioned PGPB properties within the taxa associated with the *A. halleri* rhizosphere from M
487 sites, including *Burkholderiaceae* and *Sphingomonadaceae*. For instance, the *Pandoraea*
488 genus of *Burkholderiaceae* is known to produce the enzyme 1-aminocyclopropane-1-
489 carboxylate (ACC) deaminase that alleviates stress by lowering ethylene concentrations in
490 plants exposed to biotic and abiotic stress (Anandham *et al.*, 2008). Genera of
491 *Sphingomonadaceae* can produce phytohormones like gibberellins, abscisic acid, indole-3-
492 acetic acid, and salicylic acid to promote plant growth (Yang *et al.*, 2014). Taken together, the
493 production of phytohormones and enzymes by rhizospheric PGPB are important adaptive
494 strategies that are likely to facilitate the success of *A. halleri* survival and growth in M soils.

495 The fungal taxa identified as most likely to explain differences between *A. halleri*
496 rhizosphere and surrounding background soils were almost 6-fold higher in M than in NM
497 sites (57 vs. 11 fungal taxa). Out of 57 unique rhizosphere fungal taxa associated with M sites,
498 the existing literature characterizes very few with defined functional roles to support plants.
499 Indeed, previous efforts that have characterized fungi in M soils and described fungal metal-
500 tolerance mechanisms did not report on many of the specific taxa identified in our study
501 (Miransari, 2010; Zarei *et al.*, 2010; Miransari, 2011; Luo *et al.*, 2014; Thijs *et al.*, 2017).
502 Exceptions include selected species of the genera *Hormonema* and *Phialocephala* which were

503 reported to produce the auxin phytohormone indole-3-acetic acid and siderophores,
504 respectively (Bartholdy *et al.*, 2001; Soto *et al.*, 2019). Given the number of novel fungal taxa
505 that we found in the *A. halleri* rhizosphere from M sites, but not NM sites, the importance of
506 fungi in Zn uptake (Fig. 3), and the unknown functional role of most of these taxa, further
507 research is needed to unravel their potential roles in the rhizosphere of metal-
508 hyperaccumulating plants.

509

510 *4.3 Zn and Cd hyperaccumulation are shaped by different biotic and abiotic parameters*

511 We observed a large variability in the capacity for hyperaccumulation of Zn and Cd in
512 M and NM populations of *A. halleri* from Southern Poland. While such behavior is well
513 documented in the literature, the factors that drive this variation are not yet well-understood
514 (Honjo & Kudoh, 2019). Recent studies have linked the concentration of Zn and Cd
515 accumulated in plant shoots with soil element composition showing that soil metal
516 concentrations explain only a small part of the variation in both hyperaccumulation traits
517 (Stein *et al.*, 2017; Frérot *et al.*, 2018). To further investigate factors important for Zn and Cd
518 hyperaccumulation this study measured 95 abiotic and biotic parameters. Results show that
519 Zn hyperaccumulation was predominantly governed by biotic variables and similar factors
520 were associated with both Zn shoot accumulation and the Zn translocation factor.
521 Specifically, the strongest positive association of Zn hyperaccumulation was with fungal
522 richness and diversity. This was followed by abiotic factors including ammonium N, total
523 organic C, and total N. The strongest negative associations of Zn hyperaccumulation were
524 with nitrate N and some bacterial taxa. In contrast with Zn, Cd hyperaccumulation was
525 primarily explained by abiotic factors and different factors were more strongly associated
526 with either Cd shoot accumulation or the Cd translocation factor. The strongest positive
527 association of Cd in shoot tissues was with the bioavailability of Cd, Zn, and Pb. Similarly,

528 concentrations of Cd and Pb in soil were previously reported to be strong drivers of the
529 evolution of Cd hyperaccumulation in *A. halleri* (Frérot *et al.*, 2018). Also strongly positively
530 associated with Cd in shoot tissues were several bacteria/archaea taxa which are discussed
531 further below. The variables with the strongest positive association with Cd_{TF} were a single
532 fungal taxon, and three abiotic variables including soil Cu concentration, ammonium N, and
533 total organic C.

534 Recall that Cd was hyperaccumulated only at M sites. Several bacterial taxa that were
535 abundant in the *A. halleri* rhizosphere at both M sites, but not at the NM sites, were strongly
536 associated with Cd hyperaccumulation. These include: *Actinomycetospora*, *Bradyrhizobium*,
537 *Marmoricola*, and *Pseudomonas*. *Pseudomonas* is a well-known PGPB and has previously
538 been reported to reduce metal-induced stress in plants at M sites (Xiao *et al.*, 2017; Honeker
539 *et al.*, 2019). Cadmium-resistant *Pseudomonas* sp. strains are capable of either leaching out
540 Cd from Cd-complexed compounds by producing organic acids or biosorbing metals by
541 releasing Cd-binding siderophores and peptides (Muehe *et al.*, 2015). Some strains have also
542 been shown to have a positive effect on the phytoextraction of Cd and Zn. Indeed, inoculation
543 with *Pseudomonas* sp. strains increased Cd accumulation and stimulated the growth of roots
544 and shoots in the Zn/Cd/Pb hyperaccumulator *Brassica napus* (Sheng & Xia, 2006;
545 Dell'Amico *et al.*, 2008; Dąbrowska *et al.*, 2017), and increased growth and Cd and Zn
546 content in Zn/Cd hyperaccumulator *Sedum alfredii* (Li *et al.*, 2007). Also *Bradyrhizobium*,
547 which is typically involved in atmospheric N fixation (Swanner and Templeton 2011), can
548 produce siderophores and thus has the potential to increase metal solubility in the rhizosphere
549 of metal hyperaccumulating plants (Asad *et al.*, 2019).

550 A second grouping of bacteria with PGPB activities includes taxa which were
551 associated with both Zn and Cd hyperaccumulation: *Rhodoplanes*, *Crossiella*, and
552 *Solirubrobacteraceae*, the latter two belonging to *Actinobacteria* phylum. While some

553 *Rhodoplanes* are known for their N-fixation potential (Zhu *et al.*, 2018), they are also capable
554 of producing plant growth hormones (indole-3-acetic acid and 5-aminolevulinic) (Sun *et al.*,
555 2015) that can alleviate metal-induced toxicity and stress in plants. *Actinobacteria* can
556 enhance plant growth and yield through the fixation of atmospheric N, the solubilization of
557 minerals such as P, K, and Zn, as well as the production of siderophores and plant growth
558 hormones.

559 Five bacterial/archaeal and fungal taxa were identified as negatively associated with
560 hyperaccumulation of Zn and Cd in the shoots. These included taxa that were abundant solely
561 in NM sites and belonged to the phylum *Acidobacteria* (order *Subgroup2*), genus *Nitrospira*
562 and *Phenylobacterium*. Their restriction to NM soils suggests that these microorganisms
563 might be sensitive to soil metal contamination. Indeed, previous studies showed that
564 *Acidobacteria*, which are involved in various soil processes, are sensitive to M soils (Bell *et*
565 *al.*, 2015). In contrast, the well-known nitrite oxidizer *Nitrospira* has previously been shown
566 to be adapted to M sites (Luo *et al.*, 2018). Regarding *Phenylobacterium*, its functional
567 relevance is currently unknown, however it was previously reported in the rhizosphere of *A.*
568 *halleri* from an M soil (Muehe *et al.*, 2015).

569 Finally, we note a group of 10 bacterial taxa that were present at both M sites
570 (M_PL27 and M_PL22) and at the lowland NM site (NM_PL14), but not at NM_PL35. Given
571 the remarkably high Zn hyperaccumulation levels in plants from NM_PL14, M_PL27 and
572 M_PL22 locations, these microbial taxa may play a role in the mechanism of Zn
573 hyperaccumulation. In particular, *Devosia*, which was widely abundant in our study at M and
574 NM_PL14 sites, is a well-known N-fixing bacteria (Laranjo *et al.*, 2014). *Devosia* has
575 previously been associated with Zn hyperaccumulator *Thlaspi caerulescens* (Lodewyckx *et*
576 *al.*, 2002) and Ni hyperaccumulator *Alyssum murale* (Lopez *et al.*, 2017). It has been shown
577 to occur in both bulk and rhizosphere soils at higher pH (5.2-7.8), but was present exclusively

578 in the rhizosphere of acidic soils (Honeker *et al.*, 2019). Accordingly, *Devosia* seems to be
579 recruited by plants-root systems that encounter toxic conditions and is likely to be a relevant
580 member of the rhizobacterial community associated with hyperaccumulating plants. Other
581 interesting taxa observed were *Lysinimonas* and *Galbitalea* from the *Microbacteriaceae*
582 family. Strains of these metal-resistant bacteria were isolated from the rhizosphere of *Salix*
583 *caprea* grown at a M site. They were shown to significantly increase the extractability of Zn
584 and Cd from contaminated soil and cause an increase of Zn and Cd concentration in *S. caprea*
585 shoots (Kuffner *et al.*, 2008; De Maria *et al.*, 2011). Finally, members of *Chitinophagaceae*
586 were found in both M sites and in NM_PL14. Recent research identified *Chitinophagaceae* in
587 the rhizosphere of Zn/Cd hyperaccumulator *Sedum alfredii* and showed a positive correlation
588 with Cd and Pb concentration in plant shoots and roots (Cao *et al.*, 2020). Overall, the
589 presence and ecological function of *A. halleri* rhizosphere taxa in both M sites and NM_PL14
590 (but not NM_PL35) suggests that selected members of microbial communities may affect Zn
591 and Cd mobilization in soils and result in exceptionally efficient Zn uptake by *A. halleri*
592 plants at both M and NM locations. These findings highlight the importance of investigating
593 the role of rhizosphere microbial diversity in metal mobilization at M as well as NM sites.
594 Yet, the diversity and abundance of the rhizosphere microbial community as characterized by
595 DNA amplicon sequencing may vary from those of active microbial communities. As the
596 latter may differently influence metal accumulation in *A. halleri*, future studies should
597 evaluate both, DNA and RNA, and utilize RNA:DNA ratios as a proxy for microbial activity
598 (Mei *et al.*, 2016; Bowsher *et al.*, 2019; Honeker *et al.*, 2019). Similarly, assessing the
599 bioavailable fractions of a larger suit of elements may identify additional relevant variables
600 driving metal accumulation in plants.

601

602 5. CONCLUSIONS

603 This study provides new insight into the association of soil microbial populations with
604 Zn and Cd hyperaccumulation traits in *A. halleri* growing at M and NM sites. Metal
605 contamination significantly altered the structure of soil bacterial/archaeal and fungal
606 communities and influenced the number of unique taxa recruited by the *A. halleri* rhizosphere.
607 Additionally, results show that Zn hyperaccumulation was predominantly governed by biotic
608 variables, whereas variability in Cd hyperaccumulation was primarily explained by abiotic
609 factors. We have identified a group of microbial taxa that consistently associated with Zn
610 hyperaccumulation by *A. halleri*, regardless of soil metal contamination levels. These findings
611 suggest that these taxa not only increase metal mobilization in the soil and hyperaccumulation
612 by *A. halleri*, but also benefit overall plant performance. This can result in hyperaccumulation
613 of Zn even in NM sites such as NM_PL14. The identification of taxa with potential to support
614 metal hyperaccumulation is important from an applied perspective – it is a necessary step
615 towards optimizing phytoextraction of metals from soil. We highlight the importance of
616 selecting the most promising hyperaccumulating plant populations and the need to design
617 highly specific microbial inocula with distinct functional properties to aid in the
618 hyperaccumulation process. Future work should focus on: i) unraveling the functional role of
619 the herein identified microorganisms for plant metal hyperaccumulation and ii) assessing the
620 effective role of soil abiotic and biotic factors in the adaptive evolution of *A. halleri* at M and
621 NM sites, e.g., through reciprocal transplant experiments.

622

623 CRediT authorship contribution statement

624 **Priyanka Kushwaha:** Investigation, Formal analysis, Writing - original draft. **Julia W**

625 **Neilson:** Conceptualization, Formal analysis, Funding acquisition, Writing - review & editing.

626 **Raina M Maier:** Conceptualization, Funding acquisition, Writing - review & editing. **Alicja**

627 **Babst-Kostecka:** Conceptualization, Methodology, Investigation, Formal analysis, Data
628 curation, Supervision, Funding acquisition, Writing - original draft.

629

630 **ACKNOWLEDGEMENTS**

631 This work was supported by the MINIATURA2 grant financed by the National Science
632 Centre, Poland (2018/02/X/NZ8/00546), the POWROTY/REINTEGRATION programme of
633 the Foundation for Polish Science cofinanced by the European Union under the European
634 Regional Development Fund (POIR.04.04.00-00-1D79/16-01), and by the National Institute
635 of Environmental and Health Sciences Superfund Research Program (Grant P42ES04940) at
636 the University of Arizona.

637

638 **REFERENCES**

- 639 **Ali H, Khan E, Sajad MA. 2013.** Phytoremediation of heavy metals—concepts and applications.
640 *Chemosphere* **91**(7): 869-881.
- 641 **Anandham R, Indira Gandhi P, Madhaiyan M, Sa T. 2008.** Potential plant growth promoting traits
642 and bioacidulation of rock phosphate by thiosulfate oxidizing bacteria isolated from crop
643 plants. *Journal of Basic Microbiology* **48**(6): 439-447.
- 644 **Anderson MJ. 2001.** A new method for non-parametric multivariate analysis of variance. *Austral*
645 *Ecology* **26**(1): 32-46.
- 646 **Asad SA, Farooq M, Afzal A, West H. 2019.** Integrated phytobial heavy metal remediation strategies
647 for a sustainable clean environment-a review. *Chemosphere* **217**: 925-941.
- 648 **Azarbad H, Niklińska M, Laskowski R, van Straalen NM, van Gestel CAM, Zhou J, He Z, Wen C,**
649 **Röling WFM. 2015.** Microbial community composition and functions are resilient to metal
650 pollution along two forest soil gradients. *FEMS Microbiology Ecology* **91**(1): 1-11.
- 651 **Babst-Kostecka A, Schat H, Saumitou-Laprade P, Grodzińska K, Bourceaux A, Pauwels M, Frérot H.**
652 **2018.** Evolutionary dynamics of quantitative variation in an adaptive trait at the regional
653 scale: The case of zinc hyperaccumulation in *Arabidopsis halleri*. *Molecular Ecology* **27**(16):
654 3257-3273.
- 655 **Baker AJM. 1981.** Accumulators and Excluders - Strategies in the response of Plants to heavy metals.
656 *Journal of Plant Nutrition* **3**(1-4): 643-654.
- 657 **Baker AJM. 1987.** Metal tolerance. *New Phytologist* **106**(suppl.): 93-111.
- 658 **Balabane M, Faivre D, van Oort F, Dahmani-Muller H. 1999.** Mutual effects of soil organic matter
659 dynamics and heavy metals fate in a metallophyte grassland. *Environmental Pollution* **105**(1):
660 45-54.
- 661 **Bamborough L, Cummings SP. 2009.** The impact of increasing heavy metal stress on the diversity and
662 structure of the bacterial and actinobacterial communities of metallophytic grassland soil.
663 *Biology and Fertility of Soils* **45**(3): 273-280.
- 664 **Bartholdy BA, Berreck M, Haselwandter K. 2001.** Hydroxamate siderophore synthesis by
665 *Phialocephala fortinii*, a typical dark septate fungal root endophyte. *BioMetals* **14**(1): 33-42.

- 666 **Barton CJ. 1948.** Photometric analysis of phosphate rock. *Analytical Chemistry* **20**(11): 1068-1073.
- 667 **Bell TH, Cloutier-Hurteau B, Al-Otaibi F, Turmel MC, Yergeau E, Courchesne F, St-Arnaud M. 2015.**
- 668 Early rhizosphere microbiome composition is related to the growth and Zn uptake of willows
- 669 introduced to a former landfill. *Environmental Microbiology* **17**(8): 3025-3038.
- 670 **Berg J, Brandt KK, Al-Soud WA, Holm PE, Hansen LH, Sørensen SJ, Nybroe O. 2012.** Selection for Cu-
- 671 tolerant bacterial communities with altered composition, but unaltered richness, via long-
- 672 term Cu exposure. *Applied and Environmental Microbiology* **78**(20): 7438-7446.
- 673 **Bert V, Bonnin I, Saumitou-Laprade P, de Laguérie P, Petit D. 2002.** Do *Arabidopsis halleri* from
- 674 nonmetallicolous populations accumulate zinc and cadmium more effectively than those
- 675 from metallicolous populations? *New Phytologist* **155**: 47-57.
- 676 **Bert V, Macnair MR, de Laguerie P, Saumitou-Laprade P, Petit D. 2000.** Zinc tolerance and
- 677 accumulation in metallicolous and non-metallicolous populations of *Arabidopsis halleri*
- 678 (Brassicaceae). *New Phytologist* **146**: 225-233.
- 679 **Bowsher AW, Kearns PJ, Shade A. 2019.** 16S rRNA/rRNA gene ratios and cell activity staining reveal
- 680 consistent patterns of microbial activity in plant-associated soil. *mSystems* **4**(2): e00003-
- 681 00019.
- 682 **Bressan M, Roncato MA, Bellvert F, Comte G, Haichar FEZ, Achouak W, Berge O. 2009.** Exogenous
- 683 glucosinolate produced by *Arabidopsis thaliana* has an impact on microbes in the rhizosphere
- 684 and plant roots. *ISME Journal* **3**(11): 1243-1257.
- 685 **Callahan BJ, McMurdie PJ, Rosen MJ, Han AW, Johnson AJA, Holmes SP. 2016.** DADA2: high-
- 686 resolution sample inference from illumina amplicon data. *Nat Methods* **13**(7): 581-583.
- 687 **Cao X, Luo J, Wang X, Chen Z, Liu G, Khan MB, Kang KJ, Feng Y, He Z, Yang X. 2020.** Responses of soil
- 688 bacterial community and Cd phytoextraction to a *Sedum alfredii*-oilseed rape (*Brassica napus*
- 689 L. and *Brassica juncea* L.) intercropping system. *Science of the Total Environment* **723**:
- 690 138152.
- 691 **Carrascal LM, Galván I, Gordo O. 2009.** Partial least squares regression as an alternative to current
- 692 regression methods used in ecology. *Oikos* **118**(5): 681-690.
- 693 **Corso M, Schwartzman MS, Guzzo F, Souard F, Malkowski E, Hanikenne M, Verbruggen N. 2018.**
- 694 Contrasting cadmium resistance strategies in two metallicolous populations of *Arabidopsis*
- 695 *halleri*. *New Phytologist* **218**: 283-297.
- 696 **Dąbrowska G, Hryniewicz K, Trejgell A, Baum C. 2017.** The effect of plant growth-promoting
- 697 rhizobacteria on the phytoextraction of Cd and Zn by *Brassica napus* L. *International journal*
- 698 *of phytoremediation* **19**(7): 597-604.
- 699 **De Maria S, Rivelli AR, Kuffner M, Sessitsch A, Wenzel WW, Gorfer M, Strauss J, Puschenreiter M.**
- 700 **2011.** Interactions between accumulation of trace elements and macronutrients in *Salix*
- 701 *caprea* after inoculation with rhizosphere microorganisms. *Chemosphere* **84**(9): 1256-1261.
- 702 **Dell'Amico E, Cavalca L, Andreoni V. 2008.** Improvement of *Brassica napus* growth under cadmium
- 703 stress by cadmium-resistant rhizobacteria. *Soil Biology and Biochemistry* **40**(1): 74-84.
- 704 **Dietrich CC, Bilnicki K, Korzeniak U, Briese C, Nagel KA, Babst-Kostecka A. 2019.** Does slow and
- 705 steady win the race? Root growth dynamics of *Arabidopsis halleri* ecotypes in soils with
- 706 varying trace metal element contamination. *Environmental and Experimental Botany* **167**:
- 707 103862.
- 708 **Dietrich CC, Tandy S, Banaś A, Murawska K, Korzeniak U, Łopata B, Babst-Kostecka A. 2021.**
- 709 Phytoextraction efficiency of *Arabidopsis halleri* is driven by the plant and not by soil metal
- 710 concentration. *Chemosphere*: 131437.
- 711 **Farinati S, DalCorso G, Bona E, Corbella M, Lampis S, Cecconi D, Polati R, Berta G, Vallini G, Furini A.**
- 712 **2009.** Proteomic analysis of *Arabidopsis halleri* shoots in response to the heavy metals
- 713 cadmium and zinc and rhizosphere microorganisms. *Proteomics* **9**(21): 4837-4850.
- 714 **Farinati S, DalCorso G, Panigati M, Furini A. 2011.** Interaction between selected bacterial strains and
- 715 *Arabidopsis halleri* modulates shoot proteome and cadmium and zinc accumulation. *Journal*
- 716 *of experimental botany* **62**(10): 3433-3447.

717 **Farrés M, Platikanov S, Tsakovski S, Tauler R. 2015.** Comparison of the variable importance in
718 projection (VIP) and of the selectivity ratio (SR) methods for variable selection and
719 interpretation. *Journal of Chemometrics* **29**(10): 528-536.

720 **Frérot H, Hautekèete N-C, Decombeix I, Bouchet M-H, Créach A, Saumitou-Laprade P, Piquot Y,**
721 **Pauwels M. 2018.** Habitat heterogeneity in the pseudometallophyte *Arabidopsis halleri* and
722 its structuring effect on natural variation of zinc and cadmium hyperaccumulation. *Plant and*
723 *soil* **423**: 157-174.

724 **Gans J, Wolinsky M, Dunbar J. 2005.** Computational improvements reveal great bacterial diversity
725 and high metal toxicity in soil. *Science* **309**(5739): 1387-1390.

726 **Honeker LK, Gullo CF, Neilson JW, Chorover J, Maier RM. 2019.** Effect of Re-acidification on Buffalo
727 Grass Rhizosphere and Bulk Microbial Communities During Phytostabilization of
728 Metalliferous Mine Tailings. *Frontiers in Microbiology* **10**(1209).

729 **Honjo MN, Kudoh H. 2019.** *Arabidopsis halleri*: a perennial model system for studying population
730 differentiation and local adaptation. *AoB Plants* **11**(6): plz076.

731 **Huang W, Schoenau J. 1998.** Fluxes of water-soluble nitrogen and phosphorus in the forest floor and
732 surface mineral soil of a boreal aspen stand. *Geoderma* **81**(3-4): 251-264.

733 **Khan S, Hesham AEL, Qiao M, Rehman S, He JZ. 2010.** Effects of Cd and Pb on soil microbial
734 community structure and activities. *Environmental Science and Pollution Research* **17**(2): 288-
735 296.

736 **Kuffner M, Puschenreiter M, Wieshammer G, Gorfer M, Sessitsch A. 2008.** Rhizosphere bacteria
737 affect growth and metal uptake of heavy metal accumulating willows. *Plant and soil* **304**(1):
738 35-44.

739 **Kushwaha P, Neilson JW, Barberán A, Chen Y, Fontana CG, Butterfield BJ, Maier RM. 2021.** Arid
740 Ecosystem Vegetation Canopy-Gap Dichotomy: Influence on Soil Microbial Composition and
741 Nutrient Cycling Functional Potential. *Applied and Environmental Microbiology* **87**(5): 1-17.

742 **Laranjo M, Alexandre A, Oliveira S. 2014.** Legume growth-promoting rhizobia: An overview on the
743 Mesorhizobium genus. *Microbiological Research* **169**(1): 2-17.

744 **Li WC, Ye ZH, Wong MH. 2007.** Effects of bacteria on enhanced metal uptake of the Cd/Zn-
745 hyperaccumulating plant, *Sedum alfredii*. *Journal of experimental botany* **58**(15-16): 4173-
746 4182.

747 **Lodewyckx C, Mergeay M, Vangronsveld J, Clijsters H, Van Der Lelie D. 2002.** Isolation,
748 characterization, and identification of bacteria associated with the zinc hyperaccumulator
749 *Thlaspi caerulescens* subsp. *calaminaria*. *International journal of phytoremediation* **4**(2): 101-
750 115.

751 **Lopez S, Piutti S, Vallance J, Morel J-L, Echevarria G, Benizri E. 2017.** Nickel drives bacterial
752 community diversity in the rhizosphere of the hyperaccumulator *Alyssum murale*. *Soil*
753 *Biology and Biochemistry* **114**: 121-130.

754 **Luo Y, Wu Y, Wang H, Xing R, Zheng Z, Qiu J, Yang L. 2018.** Bacterial community structure and
755 diversity responses to the direct revegetation of an artisanal zinc smelting slag after 5 years.
756 *Environmental Science and Pollution Research* **25**(15): 14773-14788.

757 **Luo ZB, Wu C, Zhang C, Li H, Lipka U, Polle A. 2014.** The role of ectomycorrhizas in heavy metal stress
758 tolerance of host plants. *Environmental and Experimental Botany* **108**: 47-62.

759 **Ma Y, Oliveira RS, Nai F, Rajkumar M, Luo Y, Rocha I, Freitas H. 2015.** The hyperaccumulator *Sedum*
760 *plumbizincicola* harbors metal-resistant endophytic bacteria that improve its phytoextraction
761 capacity in multi-metal contaminated soil. *Journal of Environmental Management* **156**: 62-
762 69.

763 **Markert JA, Champlin DM, Gutjahr-Gobell R, Grear JS, Kuhn A, McGreevy TJ, Roth A, Bagley MJ,**
764 **Nacci DE. 2010.** Population genetic diversity and fitness in multiple environments. *BMC*
765 *evolutionary biology* **10**(1): 205.

766 **Mei R, Narihiro T, Nobu M, Liu WT. 2016.** Effects of heat shocks on microbial community structure
767 and microbial activity of a methanogenic enrichment degrading benzoate. *Letters in applied*
768 *microbiology* **63**(5): 356-362.

- 769 **Mendes R, Garbeva P, Raaijmakers JM. 2013.** The rhizosphere microbiome: significance of plant
770 beneficial, plant pathogenic, and human pathogenic microorganisms. *FEMS microbiology*
771 *reviews* **37**(5): 634-663.
- 772 **Mendez MO, Maier RM. 2008.** Phytostabilization of mine tailings in arid and semiarid environments -
773 An emerging remediation technology. *Environmental Health Perspectives* **116**(3): 278-283.
- 774 **Meyer C-L, Kostecka AA, Saumitou-Laprade P, Créach A, Castric V, Pauwels M, Frérot H. 2010.**
775 Variability of zinc tolerance among and within populations of the pseudometallophyte
776 *Arabidopsis halleri* and possible role of directional selection. *New Phytologist* **185**(1): 130-
777 142.
- 778 **Micallef SA, Shiaris MP, Colón-Carmona A. 2009.** Influence of *Arabidopsis thaliana* accessions on
779 rhizobacterial communities and natural variation in root exudates. *Journal of experimental*
780 *botany* **60**(6): 1729-1742.
- 781 **Miethling R, Wieland G, Backhaus H, Tebbe CC. 2000.** Variation of microbial rhizosphere
782 communities in response to crop species, soil origin, and inoculation with *Sinorhizobium*
783 *meliloti* L33. *Microbial Ecology* **40**(1): 43-56.
- 784 **Miransari M. 2010.** Contribution of arbuscular mycorrhizal symbiosis to plant growth under different
785 types of soil stress. *Plant Biology* **12**(4): 563-569.
- 786 **Miransari M. 2011.** Hyperaccumulators, arbuscular mycorrhizal fungi and stress of heavy metals.
787 *Biotechnology Advances* **29**(6): 645-653.
- 788 **Muehe EM, Weigold P, Adaktylou IJ, Planer-Friedrich B, Kraemer U, Kappler A, Behrens S. 2015.**
789 Rhizosphere microbial community composition affects cadmium and zinc uptake by the
790 metal-hyperaccumulating plant *Arabidopsis halleri*. *Applied and Environmental Microbiology*
791 **81**(6): 2173-2181.
- 792 **Nilsson RH, Larsson K-H, Taylor AFS, Bengtsson-Palme J, Jeppesen TS, Schigel D, Kennedy P, Picard**
793 **K, Gï Ockner FO, Tedersoo L, et al. 2018.** The UNITE database for molecular identification of
794 fungi: handling dark taxa and parallel taxonomic classifications. *Nucleic Acid Res* **47**(D1):
795 D259-D264.
- 796 **Oksanen J, Kindt R, Legendre P, O'Hara B, Simpson GL, Solymos P, Stevens MHM, Wagner H. 2008.**
797 The vegan package. *Community Ecology Package* **10**: 631-637.
- 798 **Patten CL, Glick BR. 2002.** Role of *Pseudomonas putida* indoleacetic acid in development of the host
799 plant root system. *Applied and Environmental Microbiology* **68**(8): 3795-3801.
- 800 **Paulson JN, Pop M, Bravo HC. 2013.** metagenomeSeq: Statistical analysis for sparse high-throughput
801 sequencing. *Bioconductor package* **1**: 191-191.
- 802 **Penrose DM, Glick BR. 2001.** Levels of ACC and related compounds in exudate and extracts of canola
803 seeds treated with ACC deaminase-containing plant growth-promoting bacteria. *Canadian*
804 *Journal of Microbiology* **47**(4): 368-372.
- 805 **Press CM, Loper JE, Kloepper JW. 2001.** Role of iron in rhizobacteria-mediated induced systemic
806 resistance of cucumber. *Phytopathology* **91**(6): 593-598.
- 807 **Quast C, Pruesse E, Yilmaz P, Gerken J, Schweer T, Yarza P, Rg Peplies J, Glö Ckner FO. 2013.** The
808 SILVA ribosomal RNA gene database project: improved data processing and web-based tools.
809 *Nucleic Acids Res* **41**(D1): D590-D596.
- 810 **Rajapaksha RMCP, Tobor-Kapton MA, Bååth E. 2004.** Metal toxicity affects fungal and bacterial
811 activities in soil differently. *Applied and Environmental Microbiology* **70**(5): 2966-2973.
- 812 **Reeves RD, Baker AJM 2000.** Metal accumulating plants. In: Raskin I, Ensley BD eds.
813 *Phytoremediation of toxic metals: using plants to clean up the environment*. New York: Wiley
814 and Sons, 193-229.
- 815 **Reimann C, Albanese S, Batista M, Bel Lan A, Birke M, Cicchella D, Demetriades A, De Vivo B, De**
816 **Vos W, Dinelli E. 2008.** EuroGeoSurveys Geochemical mapping of agricultural and grazing
817 land soil of Europe (GEMAS)-Field manual. NGU-rapport.
- 818 **Roosens NH, Willems G, Saumitou-Laprade P. 2008.** Using *Arabidopsis* to explore zinc tolerance and
819 hyperaccumulation. *Trends in Plant Science* **13**(5): 208-215.

820 **Rosatto S, Roccotiello E, Di Piazza S, Cecchi G, Greco G, Zotti M, Vezzulli L, Mariotti M. 2019.**
821 Rhizosphere response to nickel in a facultative hyperaccumulator. *Chemosphere* **232**: 243-
822 243.

823 **Sanchez G, Sanchez MG. 2012.** Package 'plsdepot'. *Partial Least Squares (PLS) Data Analysis*
824 *Methods, v. 0.1* **17**.

825 **Segata N, Izard J, Waldron L, Gevers D, Miropolsky L, Garrett WS, Huttenhower C. 2011.**
826 Metagenomic biomarker discovery and explanation. *Genome Biology* **12**(6): 1-18.

827 **Sheng X-F, Xia J-J. 2006.** Improvement of rape (*Brassica napus*) plant growth and cadmium uptake by
828 cadmium-resistant bacteria. *Chemosphere* **64**(6): 1036-1042.

829 **Shentu JL, He ZL, Zeng YY, He SY, Du ST, Shen DS. 2014.** Microbial biomass and PLFA profile changes
830 in rhizosphere of pakchoi (*Brassica chinensis* L.) as affected by external cadmium loading.
831 *Pedosphere* **24**(4): 553-562.

832 **Solís-Dominguez FA, White SA, Hutter TB, Amistadi MK, Root RA, Chorover J, Maier RM. 2012.**
833 Response of key soil parameters during compost-assisted phytostabilization in extremely
834 acidic tailings: effect of plant species. *Environmental science & technology* **46**(2): 1019-1027.

835 **Soto J, Ortiz J, Herrera H, Fuentes A, Almonacid L, Charles TC, Arriagada C. 2019.** Enhanced arsenic
836 tolerance in *Triticum aestivum* inoculated with arsenic-resistant and plant growth promoter
837 microorganisms from a heavy metal-polluted soil. *Microorganisms* **7**(9): 1-14.

838 **Stein RJ, Höreth S, de Melo JRF, Syllwasschy L, Lee G, Garbin ML, Clemens S, Krämer U. 2017.**
839 Relationships between soil and leaf mineral composition are element-specific, environment-
840 dependent and geographically structured in the emerging model *Arabidopsis halleri*. *New*
841 *Phytologist* **213**(3): 1274-1286.

842 **Sun M, Xiao T, Ning Z, Xiao E, Sun W. 2015.** Microbial community analysis in rice paddy soils irrigated
843 by acid mine drainage contaminated water. *Applied Microbiology and Biotechnology* **99**(6):
844 2911-2922.

845 **Swanner E, Templeton A. 2011.** Potential for nitrogen fixation and nitrification in the granite-hosted
846 subsurface at Henderson Mine, CO. *Frontiers in Microbiology*, **2**, 254.

847 **Talke IN, Hanikenne M, Krämer U. 2006.** Zinc-dependent Global Transcriptional Control,
848 Transcriptional Deregulation, and Higher Gene Copy Number for Genes in Metal Homeostasis
849 of the Hyperaccumulator *Arabidopsis halleri*. *Plant Physiology* **142**: 148-167.

850 **Thijs S, Langill T, Vangronsveld J 2017.** The bacterial and fungal microbiota of hyperaccumulator
851 plants: Small organisms, large influence. *Advances in Botanical Research*: Elsevier, 43-86.

852 **Tipayno SC, Truu J, Samaddar S, Truu M, Preem JK, Oopkaup K, Espenberg M, Chatterjee P, Kang Y,
853 Kim K, et al. 2018.** The bacterial community structure and functional profile in the heavy
854 metal contaminated paddy soils, surrounding a nonferrous smelter in South Korea. *Ecology*
855 *and Evolution* **8**(12): 6157-6168.

856 **Trivedi P, Leach JE, Tringe SG, Sa T, Singh BK. 2020.** Plant–microbiome interactions: from community
857 assembly to plant health. *Nature reviews microbiology* **18**(11): 607-621.

858 **Valentín-Vargas A, Neilson JW, Root RA, Chorover J, Maier RM. 2018.** Treatment impacts on
859 temporal microbial community dynamics during phytostabilization of acid-generating mine
860 tailings in semiarid regions. *Science of the Total Environment* **618**: 357-368.

861 **van der Ent A, Baker AJM, Reeves RD, Pollard AJ, Schat H. 2013.** Hyperaccumulators of metal and
862 metalloid trace elements: Facts and fiction. *Plant and soil* **362**(1-2): 319-334.

863 **Virgone K, Ramirez-Andreotta M, Mainhagu J, Brusseau ML. 2018.** Effective integrated frameworks
864 for assessing mining sustainability. *Environmental Geochemistry and Health* **40**(6): 2635-
865 2655.

866 **Walters W, Hyde ER, Berg-Lyons D, Ackermann G, Humphrey G, Parada A, Gilbert JA, Jansson JK,
867 Gregory Caporaso J, Fuhrman JA, et al. 2016.** Improved bacterial 16S rRNA gene (V4 and V4-
868 5) and fungal internal transcribed spacer marker gene primers for microbial community
869 surveys. *mSystems* **1**(1): e00009-00015.

- 870 **Xiao X, Fan M, Wang E, Chen W, Wei G. 2017.** Interactions of plant growth-promoting rhizobacteria
871 and soil factors in two leguminous plants. *Applied Microbiology and Biotechnology* **101**(23-
872 24): 8485-8497.
- 873 **Xu Y, Seshadri B, Bolan N, Sarkar B, Ok YS, Zhang W, Rumpel C, Sparks D, Farrell M, Hall T, et al.**
874 **2019.** Microbial functional diversity and carbon use feedback in soils as affected by heavy
875 metals. *Environment International* **125**(February): 478-488.
- 876 **Yang S, Zhang X, Cao Z, Zhao K, Wang S, Chen M, Hu X. 2014.** Growth-promoting *Sphingomonas*
877 *paucimobilis* ZJSH1 associated with *Dendrobium officinale* through phytohormone
878 production and nitrogen fixation. *Microbial Biotechnology* **7**(6): 611-620.
- 879 **Yeoh YK, Dennis PG, Paungfoo-Lonhienne C, Weber L, Brackin R, Ragan MA, Schmidt S, Hugenholtz**
880 **P. 2017.** Evolutionary conservation of a core root microbiome across plant phyla along a
881 tropical soil chronosequence. *Nature Communications* **8**(1).
- 882 **Zarei M, Hempel S, Wubet T, Schäfer T, Savaghebi G, Jouzani GS, Nekouei MK, Buscot F. 2010.**
883 Molecular diversity of arbuscular mycorrhizal fungi in relation to soil chemical properties and
884 heavy metal contamination. *Environmental Pollution* **158**(8): 2757-2765.
- 885 **Zhu B, Zhang X, Zhao C, Chen S, Yang S. 2018.** Comparative genome analysis of marine purple sulfur
886 bacterium *Marichromatium gracile* YL28 reveals the diverse nitrogen cycle mechanisms and
887 habitat-specific traits. *Scientific reports* **8**(1): 1-11.

888

Table 1. Geographic location, pH, bioavailable and total Zn and Cd concentrations in rhizosphere soil samples (mean \pm SD, n=3) at the four study sites. NM = non-metalliferous sites; M = metalliferous sites.

Site	Location	Latitude [°N]	Longitude [°E]	Elevation (m)	pH	Zn _{CDGT} ¹ ($\mu\text{g L}^{-1}$)	Cd _{CDGT} ¹ ($\mu\text{g L}^{-1}$)	Total Zn (mg kg^{-1})	Total Cd (mg kg^{-1})
NM_PL14	Niepołomice	50.108833	20.367467	188	5.8 \pm 0.6	12 \pm 5	0.08 \pm 0.01	127 \pm 35	0.31 \pm 0.11
NM_PL35	Kościelisko	49.287056	19.879417	927	4.5 \pm 0.3	35 \pm 33	0.17 \pm 0.06	61 \pm 28	0.2 \pm 0.1
M_PL22	Bukowno	50.282800	19.478717	339	7.3 \pm 0.1	1052 \pm 260	13 \pm 5	6068 \pm 4916	45.2 \pm 37.2
M_PL27	Galman	50.198367	19.538817	471	6.1 \pm 0.2	614 \pm 335	8.6 \pm 4.5	9401 \pm 3160	102.4 \pm 23.7

¹Zn_{CDGT} and Cd_{CDGT} = bioavailable Zn and Cd

Table 2. Number of taxa identified by linear discriminant effect size (LEfSe) analysis that explain the differences between contaminated and uncontaminated site types and between rhizosphere and background soil communities within a given site type.

Compared Sample Groups		Number of taxa in Sample Group 1 vs. Sample Group 2; (ratio)	
Sample Group 1	Sample Group 2	Bacteria/Archaea	Fungi
M (contaminated sites)	NM (uncontaminated sites)	20 vs. 5; (4)	32 vs. 19; (1.7)
Rhizosphere soil (M sites)	Background soil (M sites)	40 vs. 7; (5.7)	57 vs. 10; (5.7)
Rhizosphere soil (NM sites)	Background soil (NM sites)	24 vs. 8; (3)	11 vs. 7; (1.6)

FIGURES

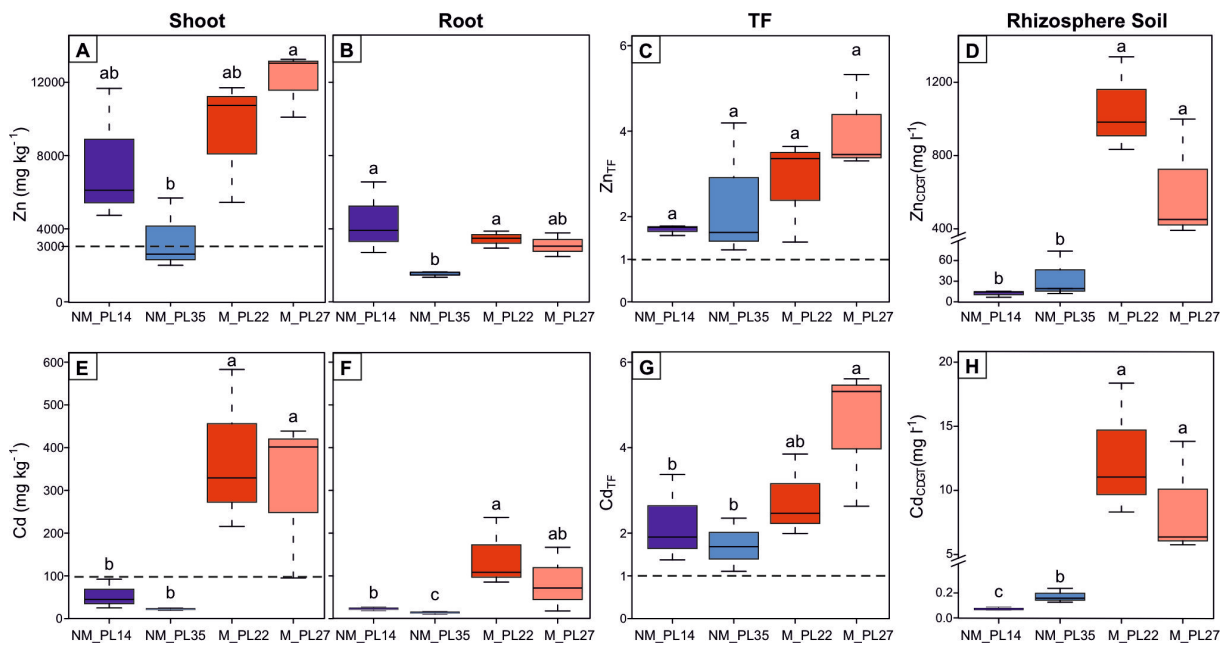


Figure 1. Uptake of Zn and Cd by *A. halleri* in the four study sites. Shoot and root concentrations of Zn (panels A and B, respectively) and Cd (panels E and F, respectively), root-to-shoot translocation factors (TF) for Zn (panel C) and Cd (panel G), and bioavailable (C_{DGT}) fractions of Zn (panel D) and Cd (panel H) in rhizosphere soil are shown for each site. Each box represents the inter-quartile range of the data, with the median indicated by the horizontal line. The dotted lines in panels A and E indicate the thresholds for hyperaccumulation for Zn and Cd, respectively. The dotted lines in panels C and G indicate a TF = 1. NM = non-metalliferous and M = metalliferous soils. Different letters indicate statistically significant differences at $p \leq 0.05$ (Kruskal-Wallis test).

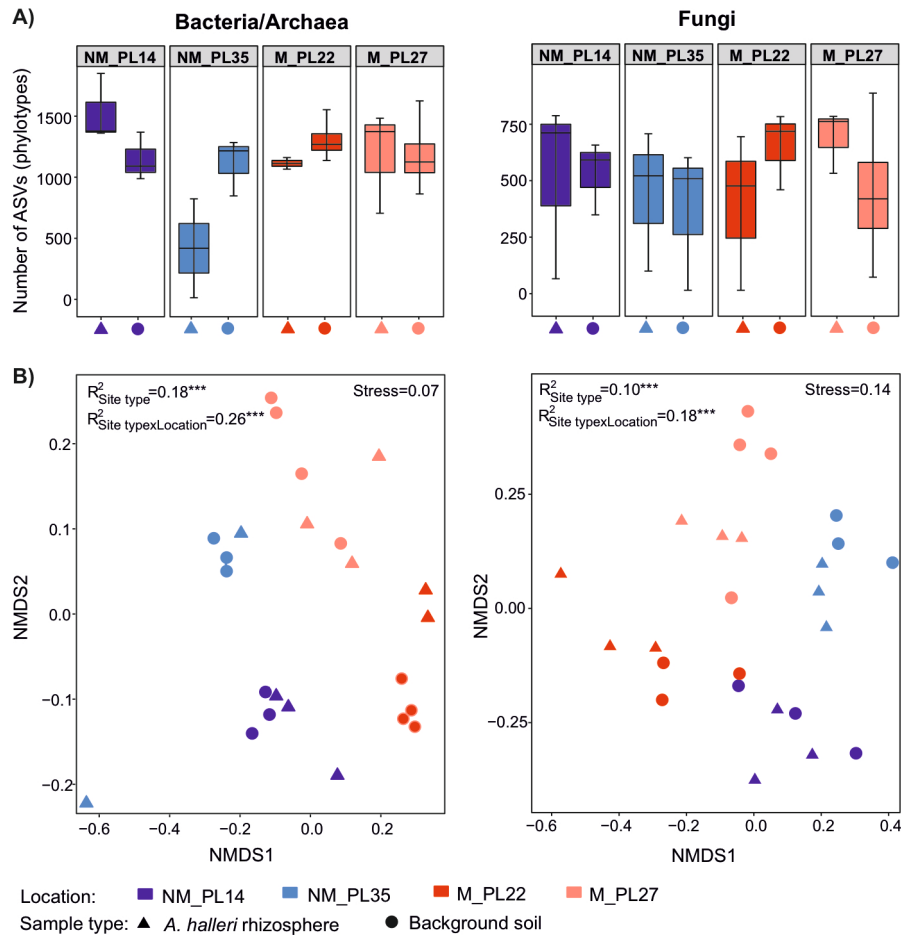


Figure 2. (A) Number of observed bacterial/archaeal and fungal amplicon sequence variants (ASVs) or phylotypes in the four study sites for rhizosphere and background soils. The boxes represent the inter-quartile range of the data, the median is indicated by the horizontal line. No comparisons between the means within the A panel were significant (Wilcoxon and Kruskal-Wallis tests). (B) Nonmetric multidimensional scaling (NMDS) ordination plots of microbial community structure in the four study sites. R^2 represents the variation explained by site type (M vs. NM) and location (NM_PL14, NM_PL35, M_PL22, M_PL27) for the microbial community composition (p -value of 0.001 is represented as ***; PERMANOVA). NM = non-metalliferous and M = metalliferous soils.

variables are highly correlated. (B) Standardized regression coefficients (St. coeff.) for explanatory variables relevant for Zn and Cd hyperaccumulation. Note that only variables with Variable Importance in Projection > 0.8 are shown. TF, translocation factor; Temp, mean annual temperature; Precip, annual precipitation; CDGT, bioavailable fractions; EC, electrical conductivity; TN, total nitrogen; TC, total dissolved carbon; TOC, total organic carbon; TIC, total inorganic carbon. The letters in front of the microbial taxa names reflect the level of taxonomic hierarchy: c, class; o, order; f, family; g, genus.

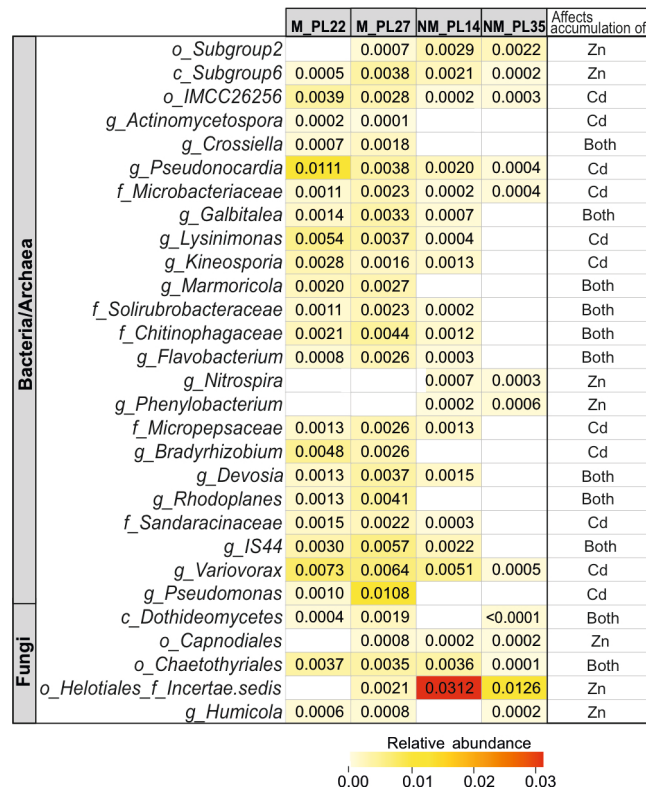


Figure 4. Heatmap showing the relative abundance of microbial taxa in *A. halleri* rhizosphere from contaminated (M_PL22, M_PL27) and uncontaminated (NM_PL14, NM_PL35) locations. The 29 taxa identified as significant drivers of Zn and Cd hyperaccumulation (as determined by partial least square regressions) were considered for the relative abundance comparison. The letters in front of the microbial taxa names reflect the level of taxonomic hierarchy: c, class; o, order; f, family; g, genus. The taxa are arranged alphabetically in the order of their phylum.